Marked suppression of In incorporation in heavily Si-doped InxGa1−xN (x 0.3) grown on GaN/α-Al2O3(0001) template

Akio Yamamoto, Akihiro Mihara, Naoteru Shigekawa, and Norihiko Narita

Additional information on Appl. Phys. Lett.
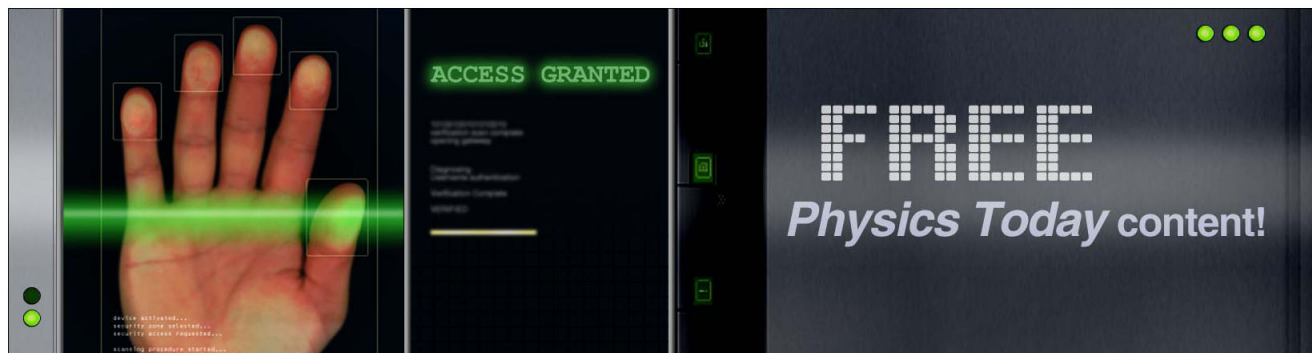
Marked suppression of In incorporation in heavily Si-doped $In_xGa_{1-x}N$ $(x \sim 0.3)$ grown on GaN/α-Al$_2$O$_3$(0001) template

Akio Yamamoto,[1,2,a] Akihiro Mihara,[1,2] Naoteru Shigekawa,[3] and Norihiko Narita[4]

[1]*University of Fukui, Fukui 910-8507, Japan*
[2]*JST-CREST, Tokyo 102-0076, Japan*
[3]*Osaka City University, Osaka 558-8585, Japan*
[4]*The Kansai Electric Power Co., Hyogo 661-0974, Japan*

$In_xGa_{1-x}N$ $(x \sim 0.3)$ films doped with Si up to $10^{22}\,cm^{-3}$ are grown on GaN/α-Al$_2$O$_3$(0001) templates by the metal-organic vapor phase epitaxy using monomethylsilane (MMSi) as a Si source. The In composition in InGaN is markedly decreased with increasing MMSi flow rate; In compositions are 0.32 and 0.12 for 0 and $4.3\,\mu$mol/min flow rates, respectively. The sum of concentrations of Si and In in InGaN is independent on MMSi flow rate and the Ga incorporation is not affected by the Si doping, suggesting that Si atoms are preferably incorporated into sites where In atoms should be incorporated. © 2013 AIP Publishing LLC. [http://dx.doi.org/10.1063/1.4819075]

InGaN ternary alloy is of great interest because of its ability to tune the direct band gap from the near infrared region of $\sim 0.7\,eV$ (InN) to the near UV region of $\sim 3.4\,eV$ (GaN). In particular, high quality In-rich InGaN alloys offer potential applications in many important areas including whole-solar-spectrum, high-efficiency multijunction tandem solar cells.[1] In a multijunction tandem cell, tunnel junction is a key part to connect sub-cells structurally and electrically. In order to realize excellent InGaN-based tunnel junctions, studies are needed on the growth of heavily impurity-doped InGaN. In III-nitrides including InGaN, Si is the most popular donor dopant. Up to now, there have been many reports on Si doping in InGaN. Several groups[2–8] have reported about the Si-doped InGaN/GaN superlattice or quantum wells, and found some favorable effects on the device performance, such as a low-operation voltage for light-emitting diodes (LEDs)[5] and a high carrier collection in InGaN quantum solar cells.[7] The Si doping was also found to improve the thermal stability of InGaN MQW.[8] There have been less numbers of reports on thick InGaN films doped with Si. Nakamura *et al.*[9] have shown the enhanced PL emission in Si-doped InGaN. Pandey *et al.*[10] have reported Si levels in InGaN with a different In content. Several groups[11–14] have found that the Si doping gives significant effects on the growth behavior of InGaN. For example, the Si doping reduces V-defects on the InGaN surface,[11] and suppresses the m-plane and c-plane slips in InGaN/GaN heterostructures.[12] Regarding the phase separation or compositional fluctuation in InGaN, Moon *et al.*[13] have reported that the Si doping suppresses the compositional fluctuations, while Li *et al.*[14] have shown that the Si doping induces the phase separation. Thus, the Si doping has pronounced effects on not only electrical and optical properties but also the growth mechanism and/or the crystal structures of InGaN.

In this paper, we report the growth behavior of metal-organic vapor phase epitaxial (MOVPE) $In_xGa_{1-x}N$ $(x \sim 0.3)$ heavily $(\sim 10^{22}\,cm^{-3})$ doped with Si. It is found that the In incorporation into grown InGaN is markedly reduced by the Si doping, while the Ga incorporation is not affected by the Si doping. This phenomenon is quantitatively analyzed using secondary ion-mass spectrometer (SIMS) data of Si in InGaN. The mechanism for the suppression of the In incorporation is discussed from the viewpoint of the length of In-N and Si-N bonds. Electrical properties of the heavily Si-doped InGaN are also shown in this paper.

The MOVPE growth of InGaN is performed at $600\,°C$ on GaN/α-Al$_2$O$_3$(0001) templates, using trimethyl-indium (TMI), triethyl-gallium (TEG), and ammonia (NH$_3$) as sources. The sheet resistance of the GaN/α-Al$_2$O$_3$(0001) template is around $2 \times 10^5\,\Omega$/sq. As a Si source, 2% monomethylsilane (MMSi) diluted by He is used. The flow rates of TMI and TEG are kept constant (7.7×10^{-6} and $2.7 \times 10^{-5}\,mol$/min, respectively), while the flow rate of MMSi is changed from 0 to $4.3 \times 10^{-6}\,mol$/min in this study. The thickness of grown InGaN films is 300–500 nm. The composition of grown films is determined from the X-ray diffraction $(2\theta/\omega)$ patterns by using the Vegard's law assuming that the films are fully relaxed. Hall measurement is performed at room temperature using van der Pauw method. As an ohmic contact to n-InGaN films, a 60 nm-thick Au is vacuum-evaporated, and then annealed in N$_2$ atmosphere at $500\,°C$ for 5 min. The optical absorption edge is measured at room temperature with a monochrometer optical system. Silicon concentrations in InGaN are measured with the SIMS (outsourced to Toray Research Center, Inc., Japan).

Figure 1 shows typical in-depth SIMS profiles of Si and In in a Si-doped InGaN grown on a GaN/α-Al$_2$O$_3$(0001) template. One can see that, across the entire InGaN film, the In composition is very uniform and Si atoms are doped very uniformly. A high concentration of C is also detected in the InGaN film. The carbon contamination level is around $1 \times 10^{20}\,cm^{-3}$ for nondoped and doped samples with MMSi flow rate of around 10 SCCM, and increases by one order of magnitude for the sample grown with a MMSi flow rate of 50 SCCM. The growth rate of InGaN is slightly increased with increasing MMSi flow rate; for example, 340 nm/h for nondoped samples and 370 nm/h for those grown with a 20–50 SCCM flow rate. Figure 2 shows the surface morphology
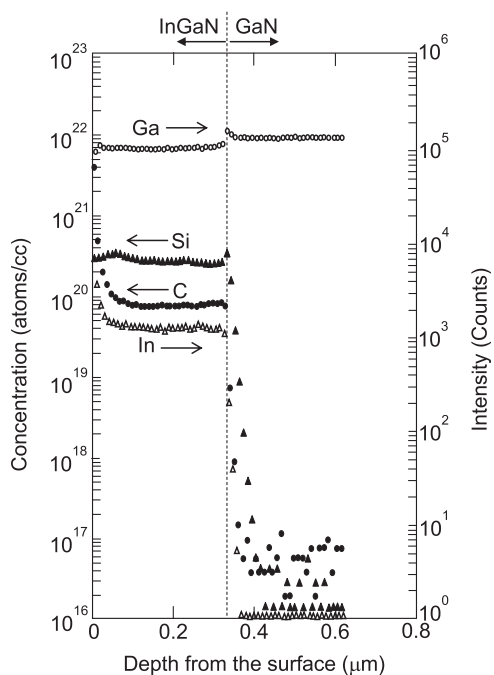
[a]Electronic mail: ayamamot@u-fukui.ac.jp

FIG. 1. Typical in-depth SIMS profiles in a Si-doped InGaN grown on GaN/α-Al₂O₃(0001) template.

FIG. 3. X-ray $2\theta/\omega$ diffraction profiles with InGaN (0002) peaks for samples grown on GaN/α-Al₂O₃(0001) template with a different MMSi flow rate.

(SEM images) of nominally undoped and Si-doped InGaN. The films show a typical surface feature of III atom-polar films. Although no marked degradation due to the Si doping is found for the surface morphology, the film grown with 4.3 μmol/min MMSi flow rate (Fig. 2(c)) shows the finer surface feature compared with that of the non-doped one (Fig. 2(a)). This indicates that the grain growth of InGaN is somewhat suppr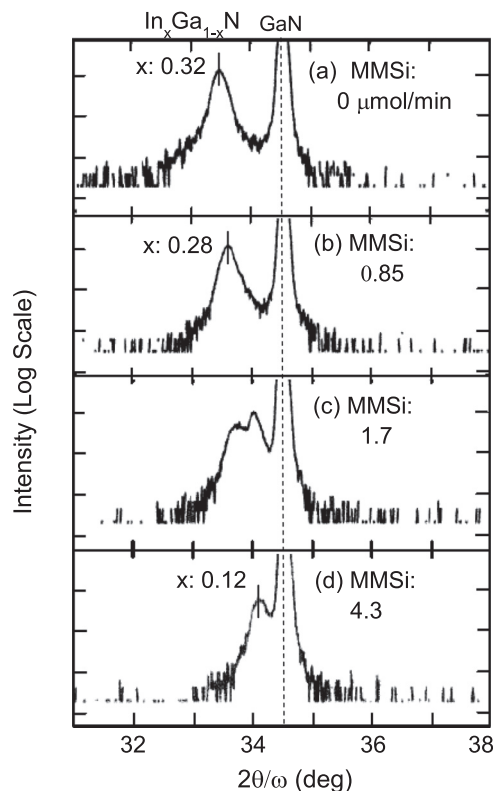essed by the Si doping with such a high Si level. Figure 3 shows the X-ray $2\theta/\omega$ diffraction profiles with InGaN (0002) peaks for samples grown on GaN/α-Al₂O₃ (0001) template with a different MMSi flow rate. The In contents shown here are obtained by using the Vegard's law assuming that the films are fully relaxed. The assumption is believed to be valid because the previous study based on the reciprocal space mapping showed that In$_x$Ga$_{1-x}$N (x $\geq$ 0.1) films with a thickness more than 300 nm grown on GaN templates were fully relaxed.[15] For the MMSi flow rate around 1.7 μmol/min, the phase separation is observed, as previously reported by Li *et al.*[14] When the MMSi flow rate is further increased, however, the phase separation is not observed. The reason for this is not clear at present. It is clearly seen in Fig. 3 that the In composition in InGaN is markedly decreased with increasing MMSi flow rate; for example, 0.32 for 0 mol/min and 0.12 for 4.3 μmol/min MMSi. Moon *et al.*[13] have observed a similar result, although the decrease of the In composition is

a few percentage. The results shown in Fig. 3 indicate that the band gap of the grown InGaN becomes large with increasing Si doping level. In order to check the band gap change, absorption coefficient for the grown films is measured at room temperature. Figure 4 shows the relationships between the square of absorption coefficient, α^2, and photon energy. The absorption edges obtained are plotted in Fig. 5 as a function of MMSi flow rate. Also shown in Fig. 5 are the In contents obtained by the X-ray diffraction and the band gap energies estimated using the In compositions and a bowing parameter b = 1.79 eV.[16] The energy gaps obtained by the both methods are in good agreement. Figure 6 shows the Si concentration [Si]$_{solid}$ in InGaN grown on GaN/α-Al₂O₃(0001) templates, obtained by SIMS analysis, as a function of MMSi flow rate. The electron concentration n and electron mobility μ obtained by the Hall measurement are also shown here. The Si concentration [Si]$_{solid}$ for the non-doped samples grown on GaN/α-Al₂O₃(0001) templates (not shown here) is around 2×10^{17} cm^{-3}. The electron concentrations in the order of 10^{20} cm^{-3} are achieved with a MMSi flow rate of around 1 μmol/min. From the ratio of n and [Si]$_{solid}$, the activation efficiency of Si

300 nm

(a) MMSi: 0 mol/min   (b) MMSi: 0.85 μmol/min   (c) MMSi: 4.3 μmol/min
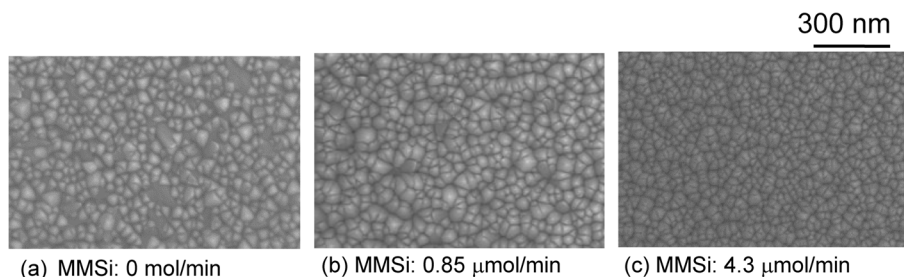
FIG. 2. Surface morphology (SEM images) of nominally undoped and Si-doped InGaN grown on GaN/α-Al₂O₃(0001) templates.

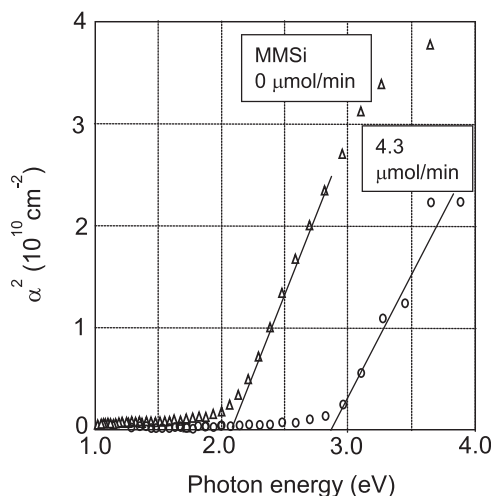FIG. 4. Photon energy dependence of square of absorption coefficient, α^2, for non-doped and Si doped InGaN.

FIG. 6. Si concentration $[Si]_{solid}$ in InGaN grown on GaN/α-Al$_2$O$_3$(0001) templates, obtained by SIMS analysis, as a function of MMSi flow rate, together with electron concentration n, and electron mobility μ obtained by the Hall measurements.

is found to be 0.16 and 0.06 for the samples with $[Si]_{solid}$ of 7×10^{20} and of 1×10^{22} cm^{-3}, respectively. The fact that an InGaN layer with a higher carrier concentration has a larger band gap is favorable to the application of Si-doped InGaN to tunnel junctions, because the optical absorption in the tunnel junction should be minimized.

In order to understand quantitatively the reduction of the In incorporation due to the Si doping, the $[Si]_{solid}$ is compared with the reduced In atoms estimated from the X-ray diffraction data. Figure 7 shows the In and Si concentrations in the grown InGaN films as a function of MMSi flow rate. With increasing MMSi flow rate, the $[Si]_{solid}$ is gradually increased, while the In concentration is decreased. The most important fact in Fig. 7 is that the sum of concentrations of Si and In is constant and independent on MMSi flow rate. From this fact, it can be concluded that the Ga incorporation is not affected by the Si doping. These results strongly suggest that Si atoms are preferably incorporated into sites where In atoms should be incorporated. Pandey et al.[10] have proposed the replacement of In by Si in InGaN, based on their results. It is known that In-N has a larger bond length (2.14 Å) than that for Ga-N (1.95 Å).[17] Therefore, the following hypothesis will arise. The incorporation of In will induce

the local compressive strain in GaN. Such a strain will tend to suppress the In incorporation. Under such a situation, Si atoms will be preferably incorporated, if they exist in the growth atmosphere, rather than In atoms. This is because Si-N has a smaller bond length (1.78–1.89 Å)[18] compared with Ga-N band. That is, the local compressive strain due to the incorporation of In-N bonds can be compensated by introducing the local tensile strain due to the incorporation of Si-N bonds. This is consistent with the previous reports showing that Si incorporation can have an effect on the microstructure of InGaN or InGaN/GaN hetrostructures.[8–14] Pandey et al.[10] have found the increase in free carrier concentration in the Si-doped InGaN with increasing In content. Such an increase in free carrier concentration may be due to the increase in Si incorporation, in addition to the decrease of Si donor level with increasing In content.[10] Aside from the hypothesis described above, there may be other mechanisms for the suppression of In incorporation. For example, gas-phase reactions between the MMSi, TMIn, TEGa, and NH$_3$ precursors could lead to a variation in the rate of formation or adsorption/desorption of various intermediate compounds as a function
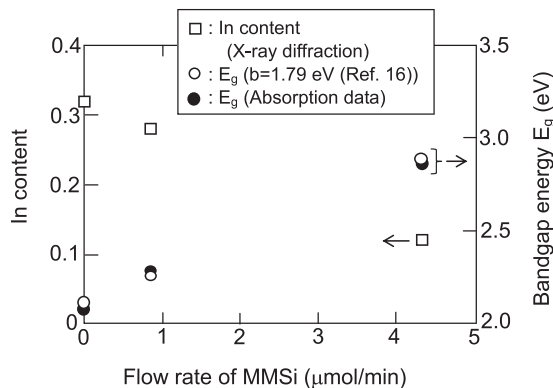

FIG. 5. Absorption edge of InGaN films as a function of MMSi flow rate. Also shown are In content obtained from X-ray diffraction and band gaps estimated using the In content and a bowing parameter b = 1.79 eV.[16]
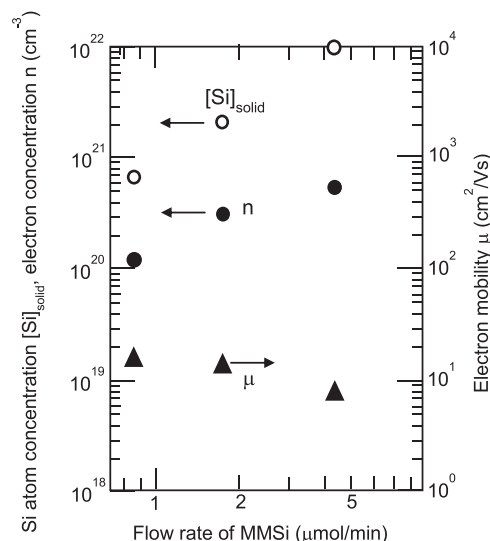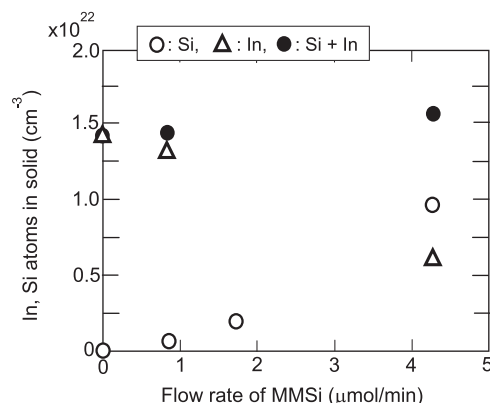

FIG. 7. In and Si atom concentrations and the sum of both in grown InGaN as a function of MMSi flow rate.

of MMSi concentration. In such a case, the growth rate of InGaN may be influenced by MMSi flow rate. However, no marked variation in the growth rate as a function of MMSi concentration is found in this study.

In summary, the MOVPE growth of heavily Si-doped InGaN is performed at $600\,^{\circ}C$ on GaN/α-Al$_2$O$_3$(0001) templates, using MMSi as a Si source. For the Si-doped samples, it is found that the In composition in InGaN is markedly decreased with increasing MMSi flow rate; In compositions are 0.32, 0.28, and 0.12 for 0, 0.85, and 4.3 μmol/min, respectively. It is found that that the sum of Si and In concentrations in InGaN is constant and independent on MMSi flow rate, and the Ga incorporation is not affected by the Si doping. This strongly indicates that Si atoms are preferably incorporated into sites where In atoms should be incorporated. Such preferential incorporation of Si and suppression of In incorporation may be related to the difference in bond length between Si-N and In-N. Electron concentrations of 10^{20}-10^{21} cm^{-3} are achieved with MMSi flow rates of $1 \sim 5\,\mu$mol/min. With increasing Si doping level, the InGaN becomes of a wider band gap material. This fact is favorable to the application of Si-doped InGaN to tunnel junctions, because the optical absorption in the tunnel junction should be minimized.

[1]A. Yamamoto, Md. R. Islam, T.-T. Kang, and A. Hashimoto, Phys. Status Solidi C **7**, 1309 (2010).

[2]T. Deguchi, A. Shikanai, K. Torii, T. Sota, S. Chichibu, and S. Nakamura, Appl. Phys. Lett. **72**, 3329 (1998).

[3]S. Chichibu, D. A. Cohen, M. P. Mack, A. C. Abare, P. Kozodoy, M. Minsky, S. Fleischer, S. Keller, J. E. Bowers, U. K. Mishra, L. A. Coldren, D. R. Clarke, and S. P. DenBaars, Appl. Phys. Lett. **73**, 496 (1998).

[4]T. Wang, H. Saeki, J. Bai, T. Shirahama, M. Lachab, S. Sakai, and P. Eliseev, Appl. Phys. Lett. **76**, 1737 (2000).

[5]J. K. Sheu, J. M. Tsai, S. C. Shei, W. C. Lai, T. C. Wen, C. H. Kou, Y. K. Su, S. J. Chang, and G. C. Chi, IEEE Electron Device Lett. **22**, 460 (2001).

[6]R.-C. Tu, C.-J. Tun, J. K. Sheu, W.-H. Kuo, T.-C. Wang, C.-E. Tsai, J.-T. Hsu, J. Chi, and G.-C. Chi, IEEE Electron Device Lett. **24**, 206 (2003).

[7]C. Neufeld, S. C. Cruz, R. M. Farrell, M. Iza, J. R. Lang, S. Keller, S. Nakamura, S. P. DenBaars, J. S. Speck, and U. K. Mishra, Appl. Phys. Lett. **98**, 243507 (2011).

[8]S.-N. Lee, J. Kim, K.-K. Kim, H. Kim, and H.-K. Kim, J. Appl. Phys. **108**, 102813 (2010).

[9]S. Nakamura, T. Mukai, and M. Senoh, Jpn. J. Appl. Phys., Part 2 **32**, L16 (1993).

[10]S. Pandey, D. Cavalcoli, and A. Cavallini, Appl. Phys. Lett. **102**, 142101 (2013).

[11]Da. -B. Li, Y.-H. Liu, T. Katsuno, K. Nakano, K. Nakamura, M. Aoki, H. Miyake, and K. Hiramatsu, Phys. Status Solidi C **3**, 1944 (2006).

[12]M. T. Hardy, E. C. Young, P. S. Hsu, D. A. Heager, I. L. Koslow, S. Nakamura, S. P. DenBaars, and J. S. Speck, Appl. Phys. Lett. **101**, 132102 (2012).

[13]Y. T. Moon, D. J. Kim, K. M. Song, I. H. Lee, M. S. Yi, D. Y. Noh, C. J. Choi, T. Y. Seong, and S. J. Park, Phys. Status Solidi B **216**, 167 (1999).

[14]N. Li, S.-J. Wang, E.-H. Park, Z. C. Feng, H.-L. Tsai, J.-R. Yang, and I. Ferguson, J. Cryst. Growth **311**, 4628 (2009).

[15]Md. R. Islam, Md. R. Kaysir, Md. J. Islam, A. Hashimoto, and A. Yamamoto, J. Mater. Sci. Technol. **29**, 128 (2013).

[16]P. G. Moses and C. G. Van de Walle, Appl. Phys. Lett. **96**, 021908 (2010).

[17]S. Sakai, Y. Ueta, and Y. Terauchi, Jpn. J. Appl. Phys., Part 1 **32**, 4413 (1993).

[18]J. Z. Jiang, H. Lindelov, L. Gerward, K. Stahl, J. M. Recio, P. Mori-Sanches, S. Carlson, M. Mezouar, E. Dooryhee, and A. Fitch, Phys. Rev. B **65**, 161202(R) (2002).